

Multiple defect model for non-monotonic structure relaxation in binary systems like Pd–Er alloys charged with hydrogen

Albert A. Katsnelson,^{1,*} Anton Yu. Lavrenov,¹ and Ihor A. Lubashevsky^{1,2}

¹*Faculty of Physics, M. V. Lomonosov Moscow State University, Moscow 119992, Russia*

²*General Physics Institute, Russian Academy of Sciences, Vavilov street 38, Moscow 119991, Russia*

(Dated: February 1, 2008)

In binary metallic systems like the Pd–Er alloys charged with hydrogen the observed structure evolution exhibits complex dynamics. It is characterized by non-monotonic time variations in an Er-rich fraction respect with an Er-poor fraction observed experimentally. The present paper proposes a qualitative model for this non-monotonic structure relaxation. We assume that the alloy have crystalline defects which trap (or emit) an additional amount of Er atoms. Hydrogen atoms into the alloy disturb the phase equilibrium as well as change the defects capacity with respect to Er atoms. Both of these factors lead to the spatial redistribution of Er atoms and cause the interface between the Er-rich and the Er-poor phase to move. The competition of diffusion fluxes in system is responsible for non-monotonic time variations, for example, in the relative volume of the enriched phase. We have found the conditions when the interface motion can change its direction several times during the system relaxation to a new equilibrium state. From our point of view this effect is the essence of the hydrogen induced non-monotonic relaxation observed in such systems. The numerical simulation confirms the basic assumptions.

I. INTRODUCTION

For the last years we obtained a series of experimental data^{1,2,3,4,5,6} showing that palladium alloys (Pd–Mo, Pd–Ta, Pd–Er, etc.) mechanically strained and also charged with hydrogen exhibit non-monotonic time variations in the phase structure during relaxation. Using X-ray diffraction techniques we studied alloys (Pd–Er in this paper) before and after the hydrogen charging. A palladium bulk was alloyed with Er of 8 atomic per cent then homogenized at temperature of 900 °C during 24 hours and quenched. Further the specimen surface was mechanically polished, thereby the superficial layer of thickness of 2–5 μm became strained. Charging the specimen with hydrogen was performed electrolytically, in 4 % NaF solute twice distilled water under current flux of 80 mA/cm² during 60 min. The X-ray diffraction picture was monitored in real time by the automatic X-ray diffractometer using monochromatic CuK_{α1} irradiation. After charging with hydrogen the palladium specimen is kept under room conditions.

At the first step we studied the Pd–Er alloy specimen after the polishing and before the charging^{1,2,3}. All the diffraction lines were of the Lorentz form in which the maximum location did not exactly correspond the face-centered cubic lattice but slightly differ to an individual distance for each diffraction maximum. This points to the presence of anisotropic elastic strains in the X-ray reflecting superficial layer that increase the spacing between the lattice planes parallel to the specimen surface. Also the diffraction maxima were slightly widened which indicate a large amount of dislocations in the reflecting layer. An evidence of the two phase state was not fixed. Peculiarities of the diffraction picture we relate to the bulk properties of the polycrystalline specimen. The grain boundaries have a minor effect because

of their small thickness.

At the initial stage of relaxation directly after charging the homogeneous alloy decomposes on two phases and a large amount of hydrogen forms and restructs crystalline defects. With time hydrogen atoms degassing the alloy keeping the structure substantially non-equilibrium. A certain amount of hydrogen remains inside the system and bounds with Pd and Er atoms and defects that allow spatial structure to evolve due to the interaction between the nonequilibrium crystalline defects and the new phase clusters. Besides, a large amount of the crystalline defects accelerates diffusion of the solute atoms promoting the microstructure evolution. For example, the vacancy concentration can attain 1–20 % inside metal–palladium alloys after charging with hydrogen (Pd–M–H systems)^{7,8,9,10}. That not only leads to the hydrogen induced atom migration but also to forming metal–hydrogen–vacancy phase.

In general the hydrogen charging changes the state of the Pd–Er alloy dramatically. Key events follow next.

First, embedded hydrogen atoms increase the lattice parameter substantially. Under relaxation the elastic strain changes from the stretching to the contraction. Then it grows during the next two days and then goes down during the further eight days decreasing for 25 %. Hereafter, as time went up to one half year, no strain variations were detected^{1,2,3}.

Second, the Lorentz form of diffraction lines now takes permanently the bimodal form.

Third, under relaxation the profile of the diffraction line exhibits quasi-periodic variations. Two components of each diffraction maximum show oscillatory changes with respect to each other. That correspond to quasi-periodic variations in the relative volume, for example, of the phase enriched with Er atoms with respect to Er-poor phase. It should be noted that changing of the phase partition changes the Er concentration in it (for

*Corresponding author. E-mail: katsnelson@lpi.ac.ru

†Present address: Institute of Metal Physics, Russian Academy of Sciences, Kosygin street 4, Moscow 117810, Russia

‡Present address: Institute of Metal Physics, Russian Academy of Sciences, Kosygin street 4, Moscow 117810, Russia

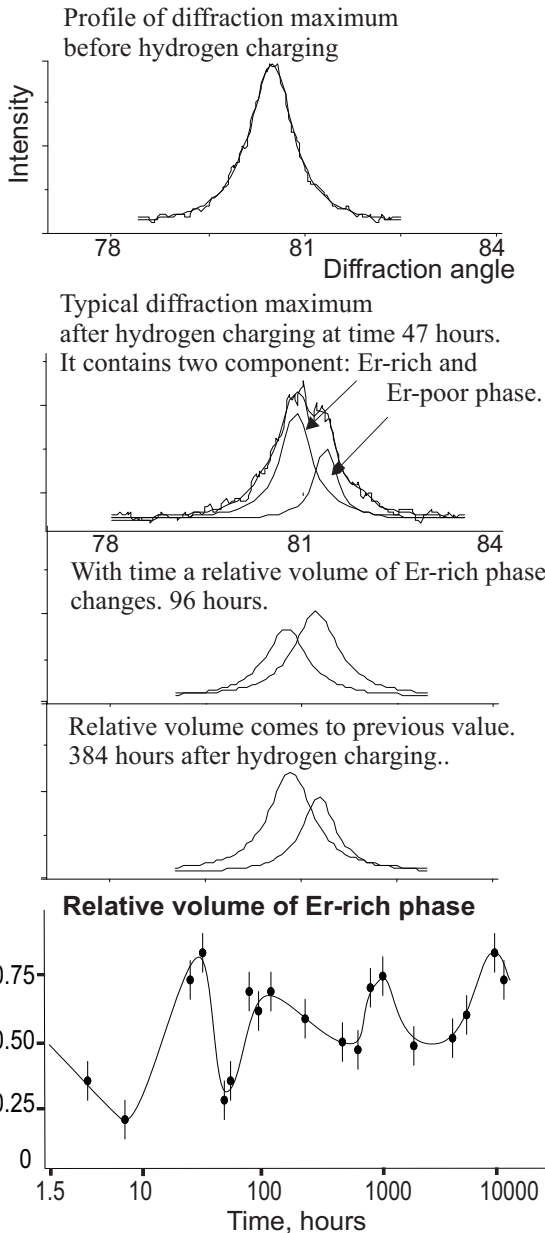


FIG. 1: Experimental data for the Pd–Er alloy (8 at. % Er).

example, the growth of Er-poor phase decreases Er concentration in it) and, as a result, the difference between Er concentrations in two phases becomes greater.

The entire phase structure of the Pd–Er alloy at different Er-concentrations is sufficiently complex¹¹ and contains many phases different in chemical composition. However we assume that corresponding phase transitions did not take place in the analyzed system because the mole fraction of Er atoms was sufficiently low, about 10 %. The observed phase structure of the Pd–Er alloy evolves the solid solution of Er atoms in the Pd matrix and an Er-rich phase which should be related in struc-

ture to the ErPd₇ intermetallic. Both of them may be modified with presence of H atoms.

We explain observed phenomena like following. First, the initial elastic strains are due to defect–metal (D–M) complexes stretching the crystalline lattice by an image forces. Hydrogen change the strain sign by the conversion of the stretching D–M complexes into contracting H–D–M ones. Indeed, due to the high bond energy of the metal–hydrogen interaction H atom should be placed inside a defect and then pulls closer metal atoms separated by the defect. The defect effective volume becomes less than the volume of the matrix crystal cell.

Second, the affinity of erbium for hydrogen is higher than that of palladium. Thereby, on one hand, the hydrogen amplifies the Er–Er interaction. That decreases the stability of the Pd–Er solid solution and leads to decomposition of homogeneous state on Er-rich and Er-poor phases. On the other hand, lattice defects (dislocations, twin boundaries, etc.) contain in nearest volume a large amount of vacancies. In presence of hydrogen these regions should attract Er atoms. In other words, the lattice defects begin to play the role of Er sink. As a result the structure evolution of the Er–Pd alloy after the hydrogen charging is governed by several factors which is responsible for the complex behavior of the system relaxation. Recently Albert Katsnelson *et al.*^{3,4} have proposed a macroscopic phenomenological model for the non-monotonic relaxation in the framework of synergetic. This paper presents a microscopic description of studied process.

II. MODEL

What is the essence of the observed phenomenon? We assume that homogeneous state of the Er–Pd alloy becomes unstable during the hydrogen charging. A large amount of hydrogen atoms promotes decomposition on Er-rich and Er-poor phases and also changes the equilibrium Er-concentrations of both phases. Also Er_xH bonds are originated because of the higher affinity of erbium for hydrogen with respect to palladium. This process amplifies the effective Er–Er attraction and changes the phase instability threshold. That makes nonequilibrium the initially formed phase regions. The further relaxation is accompanied with the phase interface motion, leading to variations, for example, in the relative volume of Er-rich phase. Caused by Er–Er attraction redistribution of Er atoms takes place first in the close vicinity of the phase interface \mathcal{T} . As a result, near the phase interface \mathcal{T} the values c_0^* and c_0 of the Er concentration in Er-rich and Er-poor phases attain new equilibrium values $c_0^*(H)$ and $c_0(H)$ depending certainly on the mean hydrogen concentration c_H in the Er–Pd alloy at the time of the experiment. The values $c_0^*(H)$ and $c_0(H)$ do not coincide with the Er concentrations inside the bulk just after the hydrogen charging. Thereby Er atoms diffuse away from the phase interface (or in opposite direction) causing the

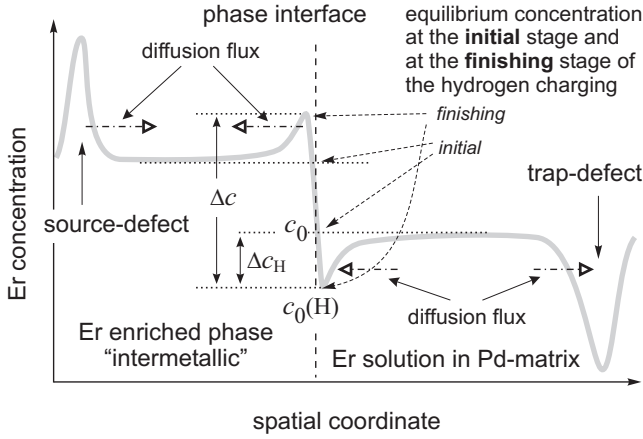


FIG. 2: Schematic illustration of the Er distribution at the beginning of the relaxation process.

interface \mathcal{T} to move. With time the Er distribution near the the interface \mathcal{T} becomes smoother and the speed of the system relaxation (interface velocity) becomes slower.

The situation is complicated by crystalline defects (Fig. 2). On one hand vacancies and theirs complexes in Er-poor phase plays the role of Er traps. On the other hand defects inside Er-rich phase can be Er atom sources. Indeed, at the initial stage of the hydrogen charging defects can attract a large amount of Er atoms originating probably not only the phase ErPd_7 but also the next phase ErPd_3 (see Ref. [11]). In equilibrium the compound ErPd_7 is intermetallic with the narrow composition interval inside which it exists. A large value of hydrogen affects the state of the compound ErPd_7 (or rigorously ErPd_xH_y where $x \approx 7$) enabling the phase exist inside more wide composition interval. In this case ErPd_3 phase can convert into the main Er-rich phase (ErPd_xH_y) releasing extra Er atoms. We see originating of an Er source. All these defects, traps and sources of Er atoms, give rise to additional diffusion fluxes competing with the diffusion fluxes induced by the phase interface. Resulting flux affects the interface motion. Exactly this flux's competition is responsible for the non-monotonic relaxation.

Let us discuss this effect in more details (with help of Fig. 2-3). At the initial stage of the hydrogen charging the chemical composition of the Er-poor phase (Er solid solution in Pd-matrix) consists of a higher value of Er concentration, c_0 , in comparison with the new equilibrium concentration $c_0(H)$ at finishing the hydrogen charging. This is due to H atoms in crystalline lattice amplify the effective Er-Er attraction. By the same reasons the opposite situation occurs in the Er-rich phase. In this phase the initial Er concentration is lower than the equilibrium concentration after the hydrogen charging. Close by the phase interface \mathcal{T} in the Er-poor phase the equilibrium values of Er concentration c_0 is constant during the motion of the interface \mathcal{T} . It is due to the fast

redistribution of Er atoms in area of the interface \mathcal{T} . The resulting distribution of Er atom and the induced diffusion flux near the interface \mathcal{T} is shown in Fig. 2. The velocity v of the interface obeys the expression

$$v \Delta c = D^* \nabla_n^* c - D \nabla_n c, \quad (1)$$

which depends only on diffusional coefficients D in each of phases and on gradients of Er-concentration close by the interface. In this formula the positive direction is shown by the axis of ordinates in Fig. 2. Δc is the drop in Er concentration c on two sides of the interface \mathcal{T} , D and D^* are the diffusion coefficients of Er atoms in Er-poor phase and Er-rich one, respectively, and, finally, the normal gradients $\nabla_n^* c$ and $\nabla_n c$ (taken at \mathcal{T}) are directed diffusion fluxes. We relate Er-rich phase to the ErPd_7 intermetallic which can exist only inside a narrow interval of chemical composition ($\nabla_n^* c$ is small). Therefore we assume the diffusion flux inside Er-poor phase (Er solid solution in the Pd-matrix) dominates the interface motion. In other words, we approximate the rigorous expression (1) as

$$v \Delta c \approx D \nabla_n c, \quad (2)$$

which focus our attention on Er-poor phase only. As follow from expression (2) the phase interface \mathcal{T} should move inwards Er-poor phase (from left to right in Fig. 2). If this phase is homogeneous then the interface motion is monotonic (without changing direction). Its speed decreases with time as the Er distribution becomes more and more uniform.

The trap-defects in Er-poor phase change the situation dramatically. Evolution of the Er distribution in the depleted phase is illustrated in Figs. 3(a)-3(d). Hydrogen activate some defects as Er atom traps. Near the defects Er concentration decreases and, as a result, takes a two-minima form shown in Fig. 3(a). If capacity of the trap is sufficiently high then with time the Er distribution will take the form shown in Fig. 3(b). In this case the Er concentration gradient $\nabla_n c$ at the interface \mathcal{T} changes the sign causing the interface \mathcal{T} to move in the opposite direction. As time goes on the defect is filled with Er atoms, the Er distribution becomes again monotonic and the interface \mathcal{T} moves in the initial direction. It should be noted that the source-defects in the Er-rich phase and the trap-defects in the Er-poor phase affect the interface motion in the same direction as it follows from Fig. 2. So we will consider only Er-poor phase. Er redistribution inside Er-rich phase cannot change essentially the results of our model. Its can change only the numerical results which are not principal for today.

Mentioned above process shows changing direction of the interface motion two time, or shows one quasi-periodic fragment of the time variations in the phase partition. At the end of this fragment teh Er distribution becomes smoother (Fig. 3(d)) and the interface velocity is less than at beginning. The following quasi-periodic fragments of the non-monotonic relaxation is due to other

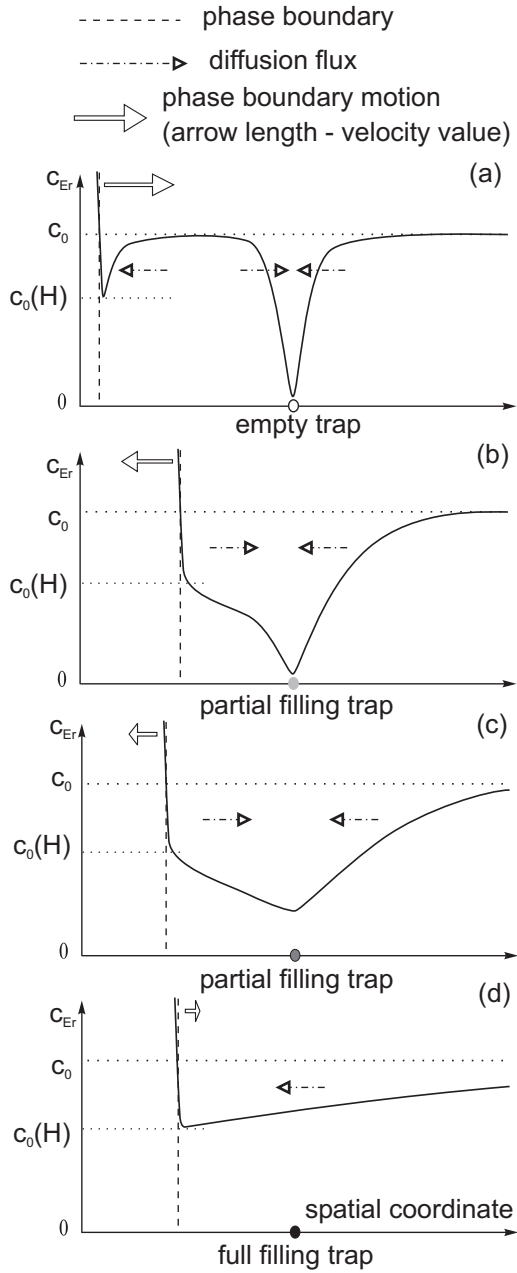


FIG. 3: Evolution of Er distribution inside Er-poor phase during the interface motion ($t_a < t_b < t_c < t_d$).

defects in the Pd-matrix. We need to develop a conception of their activation as traps or sources of Er atoms.

Before the hydrogen charging defects expand Pd-matrix and the structure of the crystalline defects should reflect this feature. Conversely after the hydrogen charging defects squeeze the lattice. Under this conditions reconstruction of the defect should take a certain time before atoms rearrange themselves. It is quite reasonable that this process meets a certain potential barrier of the lattice elasticity nature. The elastic stress caused by other defects can make this barrier higher. But when

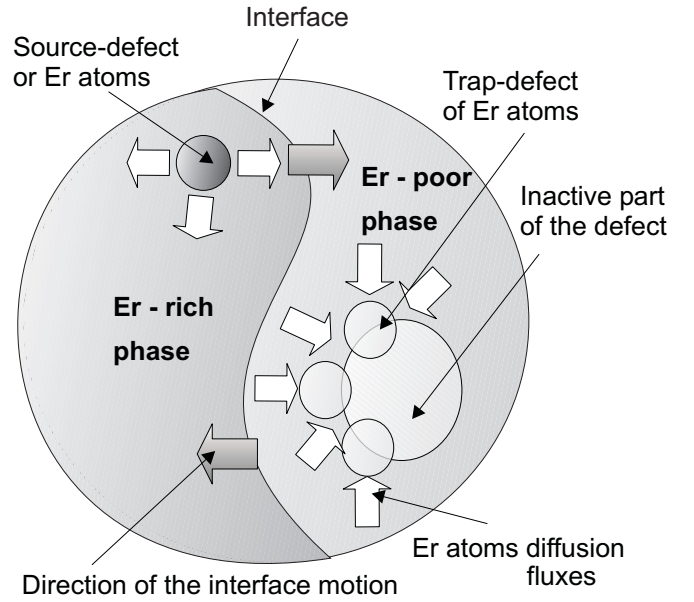


FIG. 4: Scheme of competing diffusion fluxes inside one domain of the polycrystal. The process of non-monotonic relaxation is kept by defects of different types activated at different time after hydrogen charging.

nearest defects are reconstructed completely then the potential barrier is negated because of atoms arrange its structure. In this case reconstruction of the given defect becomes more easy. From this point of view we assume that the defect will be activated as the trap of Er atom only when the preceding defect is practically filled with Er atoms. In other words, the defect activation during the interface motion proceeds like the domino effect. Each act of the defect activation and filling with Er atoms corresponds to one quasi-periodic fragment of the non-monotonic relaxation. Besides there are a number of crystalline defects of different size and kind¹⁰ which can make the relaxation even more complex. The larger is a defect, the higher is the potential barrier of atom rearrangement and, so, the more is the time needed for its reconstruction. Thereby small defects should be activated first and only then large defects can come into play (see Fig. 4). The more is the distance between the defect and the interface (or the bigger is the defect), the more is the time of Er redistribution near the interface. Therefore at the further stage of the relaxation the duration of quasi-periodic fragments is expanded remarkable.

In the present paper we will consider only characteristics of defects which are needed us for qualitative analysis. Our aim is point reader to key moments of structure evolution in Pd–Er–H system. Quantitative description is the work of future. Now we can formulate the governing equation simulating the interface motion and the non-monotonic relaxation.

III. GOVERNING EQUATIONS

Taking into account aforesaid we will consider the diffusion of Er atoms inside Er-poor phase (regarded as the half-axis $z > z_{\mathcal{T}}$) bounded by the phase interface \mathcal{T} . We write the diffusion equation for the atomic concentration c of Er atoms in this phase as

$$\frac{\partial c}{\partial t} = D \frac{\partial^2 c}{\partial z^2} - c \frac{l}{\tau_{\text{tr}}} \sum_{i=1}^{\infty}' q_i J_i(q_{i-1}) \delta(z - z_i). \quad (3)$$

Here D is the diffusion coefficient of Er atoms (which is constant in this article), the trap-defects are approximated as the δ -like sinks placed one from other at the equidistant distance $\{z_i = iz_{\text{tr}}^0\}_{i=1}^{\infty}$, and the prime means that the sum runs over all the defects located in the Er-poor phase, $z_i > z_{\mathcal{T}}$. A δ -sink is characterized by the real physical size l of a trap-defect, by the average time τ_{tr} of trapping an Er atom¹², and by the defect capacity q , i.e. the number of free seats for Er atoms at the current moment of time.

At the initial time $t = 0$ the capacities of all the defects have the same value q_0 . As time goes on the active defect i traps Er atoms decreasing the capacity q_i . We assume defect i to be activated when the capacity of the preceding defect $i-1$ drops down the threshold $q_c = \theta_c q_0$ where $\theta_c \ll 1$. This behaviour is described by the activation function for $i \geq 2$

$$J_i(q_{i-1}) = \begin{cases} 0, & \text{if } q_{i-1} \geq q_c, \\ 1, & \text{if } q_{i-1} < q_c. \end{cases} \quad (4)$$

For the first defect, by definition, $J_1 = 1$, because we assume it becomes active by the phase interface directly. The defect capacity obeys the equation

$$\frac{dq_i}{dt} = -\frac{l}{a\tau_{\text{tr}}} c(z_i) q_i J_i(q_{i-1}), \quad (5)$$

where a is the spacing of the Pd-lattice.

The phase interface \mathcal{T} initially is located at zero point

$$z_{\mathcal{T}}|_{t=0} = 0. \quad (6)$$

Its further motion is governed by the diffusion flux of Er atoms inwards the Er-poor phase and obeys the equation (see formula (2))

$$v \stackrel{\text{def}}{=} \frac{dz_{\mathcal{T}}}{dt} = \frac{D}{\Delta c} \frac{\partial c}{\partial z} \Big|_{z_{\mathcal{T}}}, \quad (7)$$

where the value Δc is shown in Fig. 2. In writing expression (7) we ignored the effect of diffusion flux inside the Er-rich phase on the interface motion. Besides when the phase interface crosses the point z_i (so defect i appears in the Er-rich phase) we assume it not affect the interface motion further. This is justified by the fact that the interface \mathcal{T} can pass through the defect location if only it is filled with Er atoms and, thus, invisible to the interface.

At the interface \mathcal{T} the Er-concentration takes the new quasi-equilibrium value which formed by fast local Er redistribution near \mathcal{T} (Fig. 2):

$$c(z_{\mathcal{T}}) = c_0 - \Delta c_{\text{H}}, \quad (8)$$

where c_0 is the initial Er-concentration inside the Pd-matrix, i.e.

$$c(z, t)|_{t=0} = c_0 \quad \text{for } z > 0. \quad (9)$$

The system of equations (3), (5), (7) with the boundary condition (8) and the initial conditions (6), (9) forms our model of the phase partition evolution or, generally speaking, the non-monotonic relaxation.

A. One quasi-periodic fragment of non-monotonic relaxation

Let us, first, find the main features of the model and write parameters (in dimensionless form) governing the structure relaxation. To do this we consider the beginning of the interface motion when the only one nearest defect is active. In the next section we will study the array of defects.

For convenience we attach our frame of reference to the moving interface. We will use in formula dimensionless time $\tau = (Dt)/(z_{\text{tr}}^0)^2$, coordinate $\xi = (z - z_{\mathcal{T}})/z_{\text{tr}}^0$, normalized Er concentration $\eta = c/c_0$, the defect capacity $\theta = q_1/q_0$ and the dimensionless time-dependent coordinate $\xi_{\text{tr}}(\tau) = (z_{\text{tr}}^0 - z_{\mathcal{T}}(t))/z_{\text{tr}}^0$ of the first defect in the moving frame. In these terms the aforesaid system is converted to the following equations:

$$\frac{\partial \eta}{\partial \tau} + \frac{d\xi_{\text{tr}}(\tau)}{d\tau} \frac{\partial \eta}{\partial \xi} = \frac{\partial^2 \eta}{\partial \xi^2} - \Omega \eta \theta \delta [\xi - \xi_{\text{tr}}(\tau)], \quad (10)$$

$$\frac{d\theta}{d\tau} = -\Lambda \Omega \eta(\xi_{\text{tr}}, \tau) \theta. \quad (11)$$

Equations (10), (11) must be completed by the boundary conditions for $\tau > 0$:

$$\left. \frac{\partial \eta(\xi, \tau)}{\partial \xi} \right|_{\xi=0} = -\frac{\Delta c}{c_0} \frac{d\xi_{\text{tr}}(\tau)}{d\tau}, \quad (12)$$

$$\eta(\xi, \tau)|_{\xi=0} = 1 - \frac{\Delta c_{\text{H}}}{c_0} \quad (13)$$

and the initial conditions:

$$\eta(\xi, \tau)|_{\tau=0} = 1, \quad \theta(\tau)|_{\tau=0} = 1, \quad \xi_{\text{tr}}(\tau)|_{\tau=0} = 1 \quad (14)$$

for $\xi > 0$. Following quantities:

$$\frac{\Delta c}{c_0}, \quad \frac{\Delta c_{\text{H}}}{c_0}, \quad \Omega = \frac{q_0 l z_{\text{tr}}^0}{D \tau_{\text{tr}}}, \quad \Lambda = \frac{c_0 z_{\text{tr}}^0}{q_0 a} \quad (15)$$

form the dimensionless parameters governing the model.

Ω is one of the key parameters of the model. If $\Omega \ll 1$ (which corresponds to small capacity of the defect q_0 or

to very fast diffusion) then the trap-defect not affect the interface motion. Lets Ω to be of order unity. At the initial stage when $\tau \ll 1$ (i.e. $t \ll (z_{\text{tr}}^0)^2/D$) the only Er redistribution near the interface T governs its dynamics. In this case the latter term on the right-hand side of Eq. (10) can be ignored and the system of equation (10), (12)–(14) has a self-similar solution:

$$\eta^*(\xi, \tau) = 1 - \sqrt{\pi} \frac{\Delta c}{c_0} \vartheta_0 e^{\vartheta_0^2} \left[1 - \text{erf} \left(\frac{\xi}{2\sqrt{\tau}} + \vartheta_0 \right) \right], \quad (16)$$

where ϑ_0 is the root of the transcendental equation:

$$\sqrt{\pi} \vartheta_0 e^{\vartheta_0^2} [1 - \text{erf}(\vartheta_0)] = \frac{\Delta c_H}{\Delta c}. \quad (17)$$

The corresponding value of the dimensionless interface velocity $\vartheta = vz_{\text{tr}}^0/D$ is written as $\vartheta = \vartheta_0/\sqrt{\tau}$. For numerical experiment we take next values: $\Delta c/c_0 = 1.5$ and $\Delta c_H/c_0 = 0.5$. In this case the value of ϑ_0 is approximately equal to $\vartheta_0 \approx 0.2$. For the given values the interface should reach the first defect (with $\Omega \ll 1$) in time $\tau \approx 10$.

Now let us activate the defect with $\Omega = 1$. As follows from Eq. (10) for a sufficiently short time $\tau \sim \Omega^{-2}$ all the Er atoms near the trap-defect will be trapped. Therefore in the vicinity of the defect Er distribution takes the form shown in Fig. 3(a). The general form of Er distribution near the defect remains unchanged until either the interface T comes close to the defect or the defect is filled with Er atoms. Certainly, the distribution width will increase with time as $\sqrt{\tau}$. From Eq. (10) for $\Omega^{-2} \ll \tau \ll 1$ Er distribution near the defect can be approximated as

$$\eta(\xi, \tau) = \text{erf} \left(\frac{|\xi - \xi_{\text{tr}}|}{2\sqrt{\tau}} \right). \quad (18)$$

Within the same time interval the dimensionless rate of trapping Er atoms by the defect is estimated as

$$\begin{aligned} & \int d\xi \Omega \theta \eta \delta(\xi - \xi_{\text{tr}}) \\ & \approx \Omega \eta(\xi_{\text{tr}}, \tau) \approx 2 \frac{\partial \eta}{\partial \xi} \Big|_{\xi=\xi_{\text{tr}}+0} \approx \frac{2}{\sqrt{\pi \tau}}. \end{aligned} \quad (19)$$

Because of diffusion dithering at time $\tau \sim 1$ Er distribution will get the form shown in Fig. 3(b). Such a distribution has a negative value of the boundary gradient, so the interface T moves in the opposite direction (according to expression (12) or (7)). As time goes on further the defect will be filled with Er atoms. The Er concentration in area of the defect will grow and the defect will affect weaker the interface motion. The corresponding form of Er distribution is illustrated in Fig. 3(c). As follows from Eq. (11) and estimate (19) the time of the defect filling is about $\tau \sim \Lambda^{-2}$. After that the defect cannot affect the interface motion. Er distribution tends again to the self-similar form (16). For observer the interface velocity changes the sing for the second time, and the

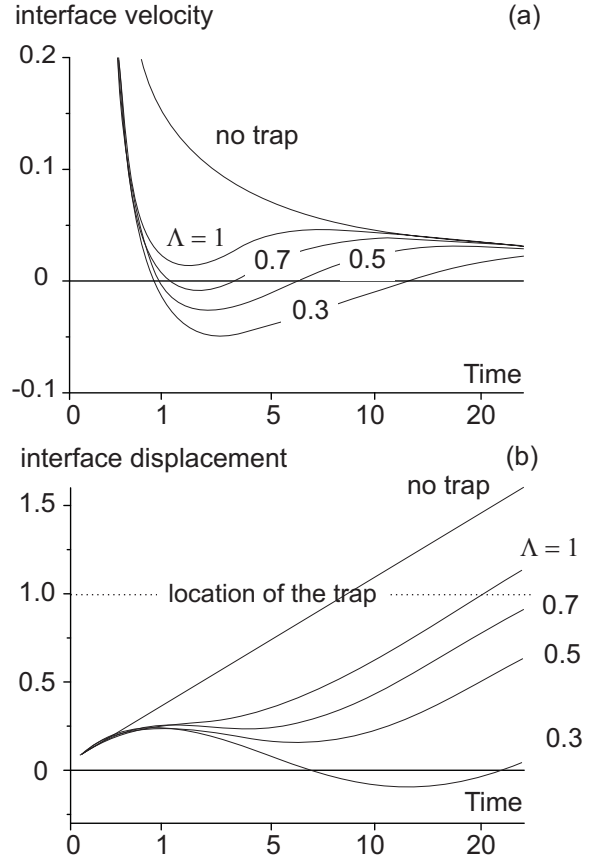


FIG. 5: The interface dynamics described by the system (10)–(14) for different values of the defect capacity. The fragment (a) shows the dimensionless interface velocity *vs* time and the fragment (b) illustrates the time dependence of the interface displacement. The abscissa exhibits time at root-square-law scale. In numerical simulation we used: $\Delta c/c_0 = 1.5$, $\Delta c_H/c_0 = 0.5$, and $\Omega = 1$. The values of the parameter Λ are pointed out at the curves.

interface motion returns to the initial direction until the next trap-defect is activated.

The aforementioned scenario describes one quasi-periodic fragment of the non-monotonic structure relaxation. For numerical analysis of (10)–(14) we take $\Delta c/c_0 = 1.5$, $\Delta c_H/c_0 = 0.5$, $\Omega = 1$ and then vary parameter Λ (in non-mathematical words we study defects of different capacities). The results are shown in Fig. 5. When the capacity of the defect is sufficiently high ($\Lambda \leq 1$) we obtain an essential backward interface motion. Otherwise, the trap-defect will be filled before the induced diffusion flux could affect the interface motion.

When the first defect is practically filled with Er-atoms the next defect will be activated. That should give rise to a similar one quasi-periodic fragment of the non-monotonic relaxation, which is the subject of the next section.

B. Multi defect effect on the interface dynamics

In this section we will use the same dimensionless time τ , coordinate ξ , the normalized Er concentration η and defect capacities $\{\theta_i = q_i/q_0\}$. In these terms the initial system of governing equations is reduced, first, to the diffusion equation written in the form

$$\frac{\partial \eta}{\partial \tau} - \vartheta \frac{\partial \eta}{\partial \xi} = \frac{\partial^2 \eta}{\partial \xi^2} - \Omega \eta \sum_{i=1}^{\infty}' \theta_i J_i(\theta_{i-1}) \delta[\xi - \xi_i(\tau)], \quad (20)$$

where according to (4) for $i \geq 2$

$$J_i(\theta_{i-1}) = \begin{cases} 0, & \text{if } \theta_{i-1} \geq \theta_c, \\ 1, & \text{if } \theta_{i-1} < \theta_c, \end{cases} \quad \text{and} \quad J_1 = 1.$$

In expression (20) the value $\vartheta = v z_{\text{tr}}^0 / D$, as before, is the dimensionless velocity of the interface \mathcal{T} and the sum runs over all the defects located inside the Er-poor phase (whose coordinates $\xi_i(\tau) > 0$ are positive in the frame attached to the moving interface \mathcal{T}). By definition $\xi_i(\tau) = i - z_{\mathcal{T}}(\tau)/z_{\text{tr}}^0$ all the quantities $\xi_i(\tau)$ changes with time at the same rate

$$\frac{d\xi_i(\tau)}{d\tau} = -\vartheta. \quad (21)$$

Second, the defects filling is described by the system of equations

$$\frac{d\theta_i}{d\tau} = -\Lambda \Omega \eta(\xi_i(\tau), \tau) \theta_i J_i(\theta_{i-1}). \quad (22)$$

Third, the interface velocity ϑ relates with the boundary condition as (12):

$$\left. \frac{\partial \eta(\xi, \tau)}{\partial \xi} \right|_{\xi=0} = \frac{\Delta c}{c_0} \vartheta. \quad (23)$$

The boundary condition (13) holds. The initial condition (14) should be replaced by the following one

$$\eta(\xi, \tau)|_{\tau=0} = 1, \quad \theta_i(\tau)|_{\tau=0} = 1, \quad \xi_i(\tau)|_{\tau=0} = i \quad (24)$$

for $\xi > 0$.

The system of equations has been analyzed numerically for the same values of the parameters $\Delta c/c_0 = 1.5$, $\Delta c_{\text{H}}/c_0 = 0.5$ but with fixed the value of the parameter Λ equal to $\Lambda = 0.5$. In other words here we fix the defect capacity and analyze the interface dynamics depending on Er diffusivity and the threshold value θ_c . At first we set $\theta_c = 10^{-4}$ and $\Omega = 2$. The corresponding dynamics of the interface \mathcal{T} is shown in Fig. 6. Similar non-monotonic structure evolution is observed for $\Omega \sim 1$. When the parameter Ω takes sufficiently large values (i.e. if the Er diffusivity D is small enough) so that $\Omega \gg 1$ then the trap-defects affect the interface motion as one trap but of much higher capacity. For example, Fig. 7

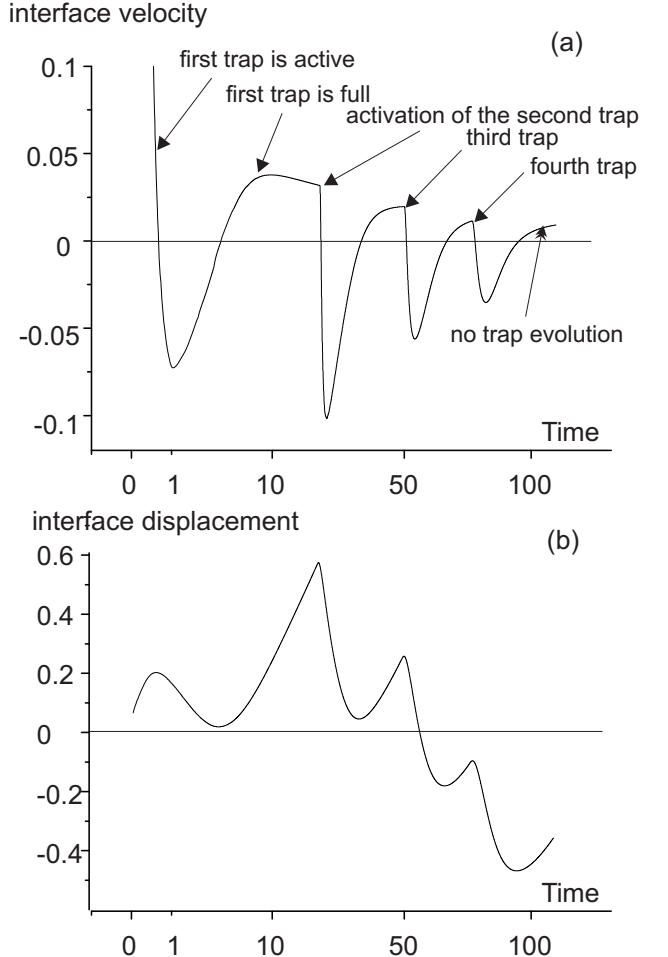


FIG. 6: Dynamics of the interface \mathcal{T} described by the system (20)–(24) in which the interface motion is affected by four trap-defects activated sequentially. The fragment (a) shows the dimensionless interface velocity *vs* time and the fragment (b) illustrates the corresponding time dependence of the interface displacement. The abscissa exhibits time at root-square-law scale. In numerical simulation we used the following values of parameters $\Delta c/c_0 = 1.5$, $\Delta c_{\text{H}}/c_0 = 0.5$, $\Lambda = 0.5$, $\theta_c = 10^{-4}$, and set $\Omega = 2$.

exhibits the interface dynamics for $\Omega = 10$. In the given case the interface motion looks like one quasi-periodic fragment but prolonged substantially. For $\Omega \ll 1$, i.e. when the Er diffusion is sufficiently fast the defects will be filled also fast and they have no considerable effect on the interface motion.

The specific details of the interface dynamics depend on the threshold θ_c of the defect activation. In particular, for $\theta_c = 10^{-2}$ we observe the interface dynamics similar to Fig. 6 for $\Omega = 1$ whereas the value $\Omega = 2$ got us to the interface motion of the same form as shown in Fig. 7.

It should be noted that in Fig. 5–7 the abscissa is a time at root-square-law scale in order to emphasize the oscillatory behaviour of the non-monotonic structure relaxation. In reality each following quasi-periodic fragment

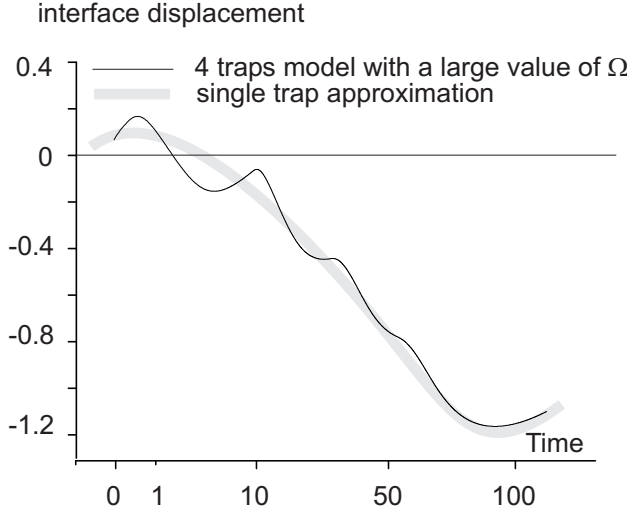


FIG. 7: Dynamics of the interface when the Er diffusion is fast. It shows the interface displacement *vs* time predicted by the system (20)–(24) when the interface motion is affected by four trap-defects activated sequentially. The abscissa exhibits time at root-square-law scale. In numerical simulation we used the following values of parameters $\Delta c/c_0 = 1.5$, $\Delta c_H/c_0 = 0.5$, $\Lambda = 0.5$, $\theta_c = 10^{-4}$, and set $\Omega = 10$.

is more prolonged than the preceding one. A similar behaviour was found experimentally (see Fig. 1). However, the experimental curve exhibits quasi-periodic time variations at logarithmic scale rather than root-square scale for the theoretical curve. We explain this discrepancy by taking into account different size of defects. When the larger a defect is, the later it comes into play and the longer time it will be filled with Er.

IV. CONCLUSION

We have proposed a mechanism which responsible for the nonmonotonic structure relaxation observed in

metallic binary systems like the Pd–Er alloys after hydrogen charging. The observed quasi-periodic alterations of the diffraction line profile are related with time variations of volume and concentration of two phase (Er-rich and Er-poor) arose in the alloy after hydrogen charging. We developed the model in which we consider active crystalline defects that trap additional amount of Er atoms. The key point of the model is disturbance by hydrogen the phase equilibrium as well as change the defect capacity with respect to Er atoms. Both of these factors lead to the spatial redistribution of Er atoms causing the interface to move between the two phases. Because of the induced diffusion fluxes these factors individually would move the interface in the opposite directions. As a result their competition is responsible for non-monotonic time variations, for example, in the relative volume of Er-rich phase observed experimentally.

We have found the conditions when the interface motion can change its direction several times during the system relaxation to a new equilibrium state. The latter effect is, from our point of view, the essence of the hydrogen induced non-monotonic relaxation observed in such systems. The numerical simulation confirms the basic assumptions.

It should be also noted that the present paper pretends only to a qualitative description of the observed non-monotonic structure relaxation. Actually we have singled out the basic feature of such systems that is responsible for this complex process. To compare the experimental data with results of numerical simulation a more sophisticated model should be developed.

Acknowledgments

This work was supported by the Russian Foundation of Basic Research, grants # 02-02-16537, # 01-01-00389 and # 02-02-06167, and by the INTAS, grant # 00-0847.

* Electronic address: albert@solst.phys.msu.su

¹ V. M. Avdjukhina, A. A. Katsnelson, and G. P. Revkevich, *Crystallogr. Rep.*, **44**, n. 1, 49 (1999).

² V. M. Avdjukhina, A. A. Katsnelson, and G. P. Revkevich, *Surf. Invest.*, n. 2, 34 (2001).

³ A. A. Katsnelson, V. M. Avdjukhina, and G. P. Revkevich, *Surf. Invest.*, n. 2, 39 (2001).

⁴ A. A. Katsnelson, V. M. Avdjukhina, D. A. Olemskoi, A. I. Olemskoi, and G. P. Revkevich, *Phys. Met. Met.* **88**, n. 6, 63 (1999).

⁵ V. M. Avdjukhina, A. A. Katsnelson, G. P. Revkevich, Khan Kha Sok, *et al.*, International Scientific Journal for Alternative Energy and Ecology, **1**, 11 (2000).

⁶ V. M. Avdjukhina, A. A. Anishchenko, A. A. Katsnelson, and G. P. Revkevich, *Perspekt. Mat.*, n. 6, 52 (2002) (in

Russian).

⁷ G. P. Revkevich, A. A. Katsnelson, V. M. Khristov, M. A. Knyazeva, *Izvestiya Akad. Nauk USSR (metals)*, n. 4, 180 (1990) (in Russian)

⁸ Fukai Y., Okuma N., *Phys.Rev.Lett.*, v.73, 1640 (1995). Fukai Y., J. All. Comp., v. 231, 35 (1994).

⁹ V. M. Avdjukhina, A. A. Katsnelson, G. P. Revkevich, Khan Kha Sok, A. V. Knyaginichev, *Crystallogr. Rep.*, **47**, n. 3, 393 (2002).

¹⁰ V. M. Avdjukhina, A. A. Anishchenko, A. A. Katsnelson, and G. P. Revkevich, *Perspekt. Mat.*, n. 4, 11 (in Russian).

¹¹ Z. Du and H. Yang, *J. Alloys Comp.*, **299**, 199 (2000).

¹² The time τ_{tr} should not be confused with the lifetime of Er atoms inside the defect which infinitely long in the given model.